ACS APPLIED MATERIALS & INTERFACES

Research Article

www.acsami.org

Highly Transparent, Visible-Light Photodetector Based on Oxide Semiconductors and Quantum Dots

Seung Won Shin,[†] Kwang-Ho Lee,[‡] Jin-Seong Park,[‡] and Seong Jun Kang*[,†]

[†]Department of Advanced Materials Engineering for Information and Electronics, Kyung Hee University, 1732 Deogyeong-daero, Giheung-gu, Yongin, Gyeonggi-do 446-701, Republic of Korea

[‡]Division of Materials Science and Engineering, Hanyang University, 222 Wangsimni-ro, Seoul 133-719, Republic of Korea

Supporting Information

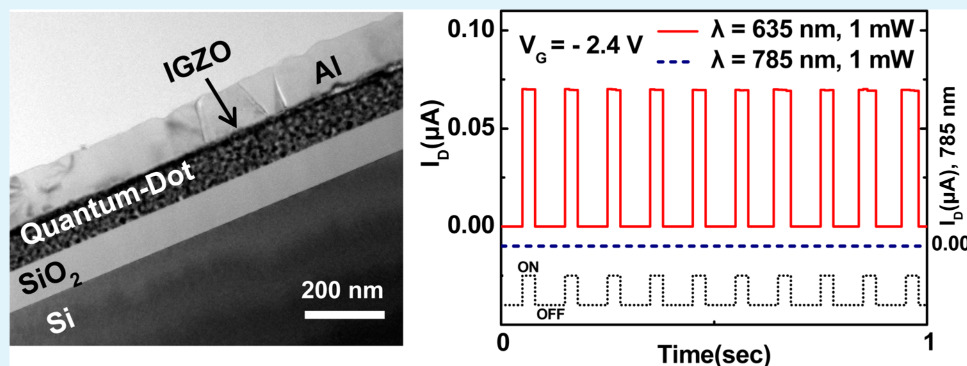

ABSTRACT: Highly transparent phototransistors that can detect visible light have been fabricated by combining indium–gallium–zinc oxide (IGZO) and quantum dots (QDs). A wide-band-gap IGZO film was used as a transparent semiconducting channel, while small-band-gap QDs were adopted to absorb and convert visible light to an electrical signal. Typical IGZO thin-film transistors (TFTs) did not show a photocurrent with illumination of visible light. However, IGZO TFTs decorated with QDs showed enhanced photocurrent upon exposure to visible light. The device showed a responsivity of 1.35×10^4 A/W and an external quantum efficiency of 2.59×10^4 under illumination by a 635 nm laser. The origin of the increased photocurrent in the visible light was the small band gap of the QDs combined with the transparent IGZO films. Therefore, transparent phototransistors based on IGZO and QDs were fabricated and characterized in detail. The result is relevant for the development of highly transparent photodetectors that can detect visible light.

KEYWORDS: *IGZO, cadmium selenide, quantum dots, photodetector, visible light, transparent photodetector*

1. INTRODUCTION

Oxide semiconductors, such as indium–gallium–zinc oxide (IGZO), are considered a good candidate to replace traditional silicon in various electronic devices.[1−3] The field-effect mobility and on/off ratio of typical IGZO thin-film transistors (TFTs) are reported to be >10 $cm^2/V{\cdot}s$ and $\sim 10^7$, which are comparable to those of amorphous silicon TFTs.[4] Moreover, oxide semiconductor devices are transparent because of their intrinsic wide-band-gap properties.[5] Therefore, oxide semiconductors are considered to be the most appropriate semiconducting materials for high-performance, transparent electronics, including logic circuits and sensors.[6,7] Recently, there have been several attempts to develop a phototransistor using transparent oxide semiconductors.[8,9] However, oxide semiconductors have been used as the phototransistor, which can convert only ultraviolet (UV) light to electrical current. The intrinsic wide band gap of an oxide semiconductor causes limitation of the absorbed light to the high-energy UV region. Chang et al. have successfully demonstrated an amorphous IGZO phototransistor with light responsivity at a wavelength of 250 nm.[8] However, the phototransistors could not respond to visible light because of the wide band gap of amorphous IGZO. This illustrates the difficulty of fabricating a transparent phototransistor that can respond to visible light using oxide semiconductors.

Several methods have been reported to improve the photoresponsivity of oxide TFTs in the visible-light region.[10,11] Polymeric absorption layers were coated onto the surfaces of IGZO films to improve the response in visible light.[10] Additionally, metal nanoparticles have been decorated with oxide semiconductors to increase the photocurrent with exposure to visible light.[11] Recently, quantum dots (QDs) have also been adopted on the IGZO film in order to improve the photoresponsivity in the visible-light region.[12] QDs have a narrow, tunable band gap in the range of visible light that can easily be controlled by changing their size.[13] Therefore,

Received: May 29, 2015
Accepted: August 21, 2015
Published: August 21, 2015

© 2015 American Chemical Society

DOI: 10.1021/acsami.5b04683
ACS Appl. Mater. Interfaces 2015, 7, 19666−19671

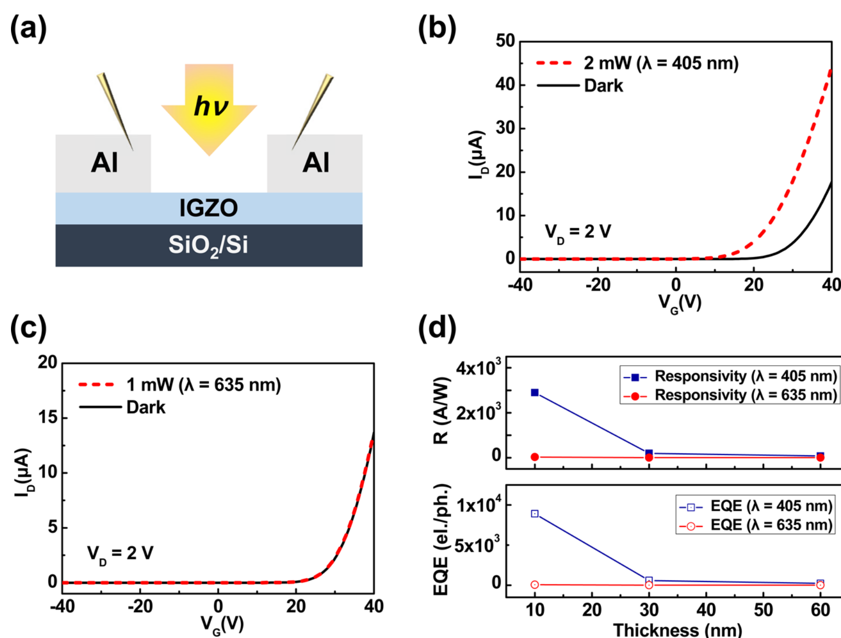

Figure 1. (a) Schematic illustration of the device and measurements. Transfer curves (V_D = 2 V and V_G = 30 V) of the device under illumination of (b) 405 and (c) 635 nm laser sources. (d) Changes in the responsivity and EQE of the devices according to the thickness of the IGZO film.

phototransistors based on oxide semiconductors and QDs have been successfully demonstrated by several research groups.[12,14] However, more investigations are necessary to determine efficient device structures for the development of highly transparent, visible-light phototransistors based on oxide semiconductors and QDs.

In this study, hybrid films of IGZO and QDs were fabricated, where QDs were placed on the top of the IGZO surface or under the IGZO film in order to determine the most efficient device structure. Additionally, the thickness of the IGZO film was controlled. The device performance according to the device structure was measured in detail by considering the photoresponsivity and external quantum efficiency (EQE). The optimized device structure, along with a detailed study of the improved photocurrent in the visible-light range, enables the fabrication of transparent phototransistors that can respond to visible light.

2. EXPERIMENTAL SECTION

2.1. Device Fabrication. IGZO films were deposited on clean SiO_2 (100 nm)/silicon (Si) substrates using a radio-frequency (RF) sputtering system with a single target of In_2O_3:Ga_2O_3:ZnO = 1:1:1 atom %. The RF power was 100 W, while the vacuum was maintained at 5 mTorr. The IGZO films were postannealed at 350 °C in ambient air for 1 h in order to control the carrier concentration.[15] A conventional photolithography process and thermal evaporator were used to fabricate the oxide TFTs, and 100 nm of aluminum was deposited as source and drain electrodes. Additionally, a buffered oxide etchant was used to define the active channel area and isolate each oxide TFT on the substrate. The IGZO TFTs had a channel length of 25 μm and a width of 200 μm with a bottom-gate structure. Colloidal cadmium selenide (CdSe) QDs (Sigma-Aldrich Lumidot CdSe-640, core-type, diameter 6.2−7.7 nm) were spin-coated onto the active channel area and annealed at 180 °C for 30 min. The device was then dipped in a 20 mM methanol solution of 1,7-diaminoheptane at 70 °C for 15 min for the cross-linking process. Finally, the device was rinsed with isopropyl alcohol and dried at 180 °C for 30 min. The same QD coating procedure was repeated on the Al_2O_3 (100 nm)/indium−tin oxide/glass substrates in order to fabricate the transparent devices, where the QDs were placed at the interface between Al_2O_3 and IGZO.

2.2. Sample Measurements. The electrical properties of the devices were measured using a semiconducting parameter analyzer (HP 4145B) and a probe station. The photoresponses of the devices were measured upon exposure to various laser sources of IR (λ = 785 nm), red (λ = 635 nm), green (λ = 532 nm), and UV (λ = 405 nm). Scanning electron microscopy (SEM) and transmission electron microscopy (TEM) were used to investigate the device structure.

3. RESULTS AND DISCUSSION

Figure 1 shows the typical device characteristics of wide-band-gap oxide TFTs. A 10-nm-thick IGZO film was deposited on the SiO_2/Si substrate with aluminum source−drain electrodes in order to fabricate bottom-gate-structured TFTs, as shown in Figure 1a. Figure 1b shows the transfer curves of IGZO TFTs with and without 405 nm laser exposure. An increase in the drain current (I_D) was clearly observed. A high-photon-energy, 405 nm laser was sufficient to induce the photocurrent on wide-band-gap IGZO TFTs. Alternatively, the photon energy of the 635 nm laser was 1.95 eV, which is smaller than the band gap of an IGZO semiconductor. Therefore, the photocurrent was not observed because of device exposure to a 635 nm laser, as shown in Figure 1c. (Figure S1 summarizes the output and transfer characteristics of IGZO TFTs with/without a 635 nm laser source, according to the thickness of the IGZO film.) Responsivity and EQE were evaluated with different laser wavelengths (λ = 405 and 635 nm) according to the thickness change of the IGZO active layer, as shown in Figure 1d.[16]

$$\text{responsivity} = \frac{(I_{\text{total}} - I_{\text{dark}})/A_{\text{pt}}}{P/A_{\text{pd}}} = \frac{J_{\text{ph}}}{P} \quad (1)$$

$$\text{EQE} = \frac{J_{\text{ph}}/q}{P/h\nu} \quad (2)$$

In eqs 1 and 2, I_{total} is the total photocurrent, I_{dark} is the dark current, P is the incident laser power, A_{pt} is the product of the channel width and thickness, A_{pd} is the spot size of the laser source, J_{ph} is the photocurrent density, and P is the incident

DOI: 10.1021/acsami.5b04683
ACS Appl. Mater. Interfaces 2015, 7, 19666−19671

laser power density. Both the responsivity and EQE of the devices with various thicknesses of IGZO were negligible after exposure to the 635 nm laser. However, the responsivity and EQE increased with exposure to a 405 nm laser with reduced thickness of IGZO, as shown in Figure 1d. Therefore, IGZO TFTs can induce a photocurrent only with a high-photon-energy, 405 nm laser source because of their wide band gap.

To increase the photoresponse under visible light, CdSe QDs were spin-coated onto the surface of IGZO, as shown in Figure 2a. The band gap of CdSe QDs was 1.83 eV, small enough to absorb visible light.[14] Figure 2b shows an SEM image of QDs uniformly distributed in the channel region of IGZO between the source and drain electrodes. The device showed typical n-type TFT behavior, and an increased I_D was clearly observed with exposure of visible light (λ = 635 nm). (Figure S2 summarizes the output and transfer characteristics of IGZO TFTs with QDs with/without a 635 nm laser source.) According to the change in the thickness of IGZO, QDs were placed at different distances from the channel regions of IGZO TFTs. The responsivity and EQE of the devices with QDs are summarized in Table 1. The highest values of the responsivity and EQE were obtained with 10-nm-thick IGZO TFTs. Because of the short distance between the active channel region and QDs, the absorbed photons effectively induce the photocurrent in the device. The photoresponses of the device with 10-nm-thick IGZO TFTs with QDs coated on the surface were also evaluated according to the laser wavelength (λ = 405, 532, 635, and 785 nm). Figure 2c illustrates that the 785 nm light source did not induce a photocurrent because the photon energy was smaller than the band gap of the QDs. With a reduction in the wavelength of the light source, the responsivity and EQE increased even under visible light, indicating that visible light induces a photocurrent in the device because of the small band gap of CdSe QDs. In the higher-photon-energy region, the responsivity and EQE values were increased because both QDs and IGZO absorb photons to increase the photocurrent. The device without the IGZO semiconducting channel, which has only QDs, was also fabricated to evaluate the photoresponsivity. However, the current level was too low (10^{-10}–10^{-11} A) because of the discontinuous film of QDs. (Figure S3 summarizes the transfer characteristics of the device, which has only QDs.)

To enhance the photocurrent of the device, QDs were inserted between 10-nm-thick IGZO and SiO_2, as shown in Figure 3a. Figure 3b shows the cross-sectional TEM image of the device, where uniformly coated QDs were clearly observed at the interface. QDs were then placed in the active channel region of the IGZO TFTs. The device showed a typical n-type behavior, and the photocurrent was observed with 635 nm visible light, as summarized in Figure S4a. The time-resolved photocurrent produced after a pulse of the 635 nm laser was

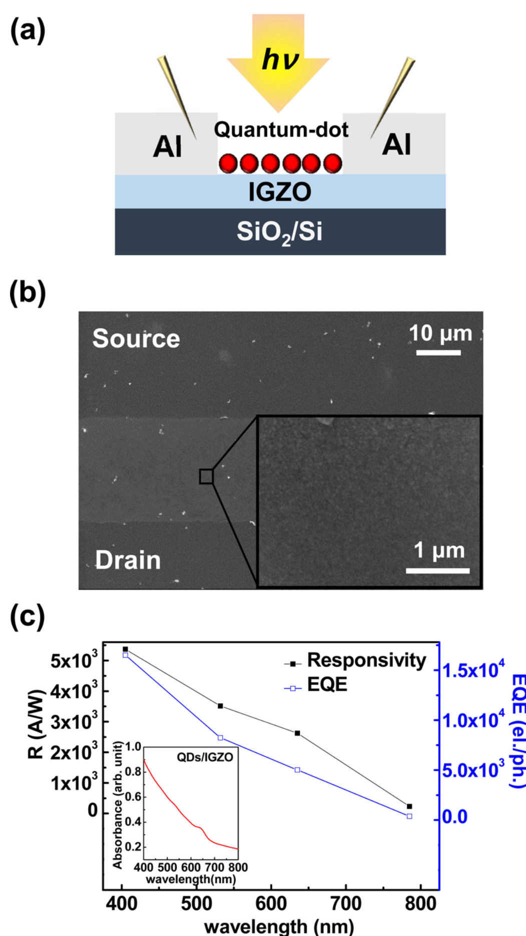

Figure 2. (a) Schematic illustration of the device with decorations of QDs on the surface of IGZO. (b) SEM image of the active channel region, where QDs are coated on the surface. (c) Changes in the responsivity and EQE according to the wavelength of the laser source (V_D = 10 V and V_G = 20 V). The inset shows the absorption spectrum of the QDs/IGZO hybrid film.

Table 1. Responsivity and EQE Values of the IGZO TFTs, Where QDs Were Decorated on Different Thicknesses of IGZO Films[a]

thickness (nm)	responsivity (A/W)	EQE (el./ph.)
10	13541.1	2.591×10^4
30	12128.1	2.321×10^4
60	6388.5	1.222×10^4

[a] The wavelength of the laser source was 635 nm (V_D = 10 V and V_G = 30 V).

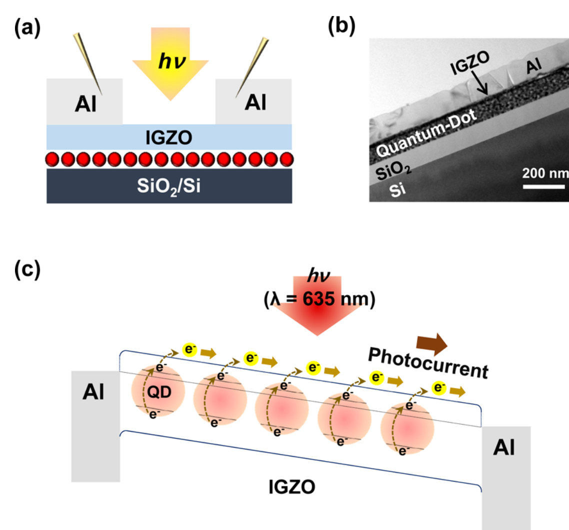

Figure 3. (a) Schematic illustration of the device, where QDs are inserted at the interface between IGZO and SiO_2. (b) Cross-sectional TEM image of the device. (c) Mechanism of the visible-light-induced photocurrent on the hybrid films of QDs and IGZO.

DOI: 10.1021/acsami.5b04683
ACS Appl. Mater. Interfaces 2015, 7, 19666–19671

also measured, as shown in Figure S4b. The time-resolved measurements showed a fast response time to visible light. Figure 3c explains the origin of the device photocurrent with exposure of visible light. Small-band-gap QDs absorb visible light, and the electrons are excited from the valence band to the conduction band of QDs. Therefore, QDs can induce and inject additional photoexcited electrons into the conduction band of IGZO even with a low-energy photon (λ = 635 nm). In this way, the photocurrent of the wide-band-gap device can be increased with visible light because of the presence of small-band-gap QDs. Figure 4 shows the time-dependent photoresponses of the device, where the QDs were placed at the interface between IGZO and SiO_2. As shown in Figure 4a, a 10 Hz laser pulse (1 mW; λ = 635 and 785 nm) was applied to the device. The photocurrent increased under illumination of the 635 nm laser and quickly decreased to a negligible value when illumination was removed. Even the photon energy (λ = 635 nm) was not sufficient to overcome the band gap of IGZO, and a quick response in the photocurrent was observed because of the small-band-gap QDs. However, the device did not show a photoresponse to the laser illumination of a low photon energy (λ = 785 nm). To quantify the photoresponse, parameter η was evaluated with eq 3.[17]

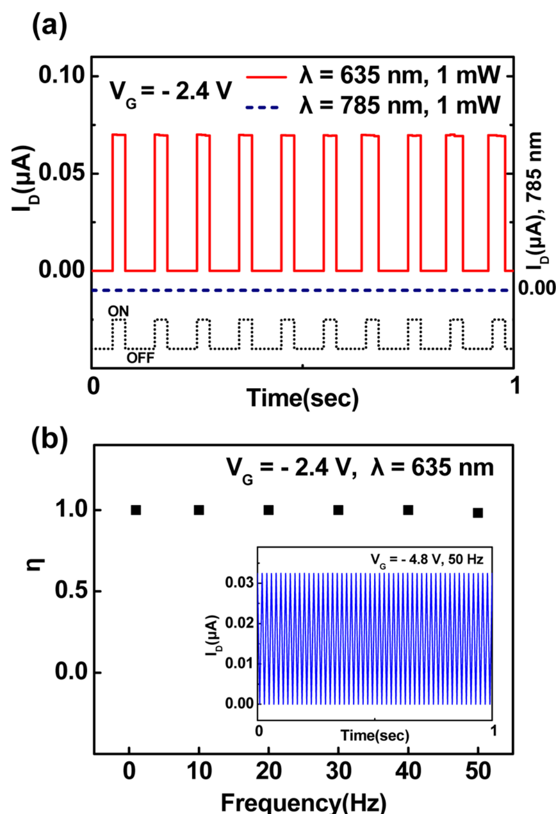

Figure 4. (a) Time-dependent photoresponses (λ = 635 and 785 nm) of the device, where QDs are inserted at the interface between IGZO and SiO_2. The on/off input signal is shown at the bottom. (b) Parameter η at different frequencies of laser light (λ = 635 nm). The inset shows the photoresponse of the drain current at the 50 Hz laser source.

$$\eta = \frac{I_{on} - I_{off}}{I_{on} + I_{off}} \qquad (3)$$

In this equation, I_{on} is the I_D with laser illumination and I_{off} is the I_D in the dark state. When the device can be completely turned on and off according to illumination, the parameter η is 1. However, the parameter is going to be smaller than 1 when the device is not working properly. Figure 4b shows parameter η as a function of the illumination frequency of the 635 nm laser. The parameter is nearly 1 up to an illumination frequency of 50 Hz, which is not a frequency visible to the human eye. The inset shows the photoresponse of the device at the 50 Hz input illumination (λ = 635 nm). Therefore, transparent visible-light phototransistors that can detect a frequency of light not visible to the human eye can be fabricated by combining QDs at the interface between IGZO and SiO_2.

Transparent phototransistors were fabricated on a glass substrate, as shown in Figure 5a. The device had a hybrid active channel region of 10-nm-thick IGZO and QDs, where QDs

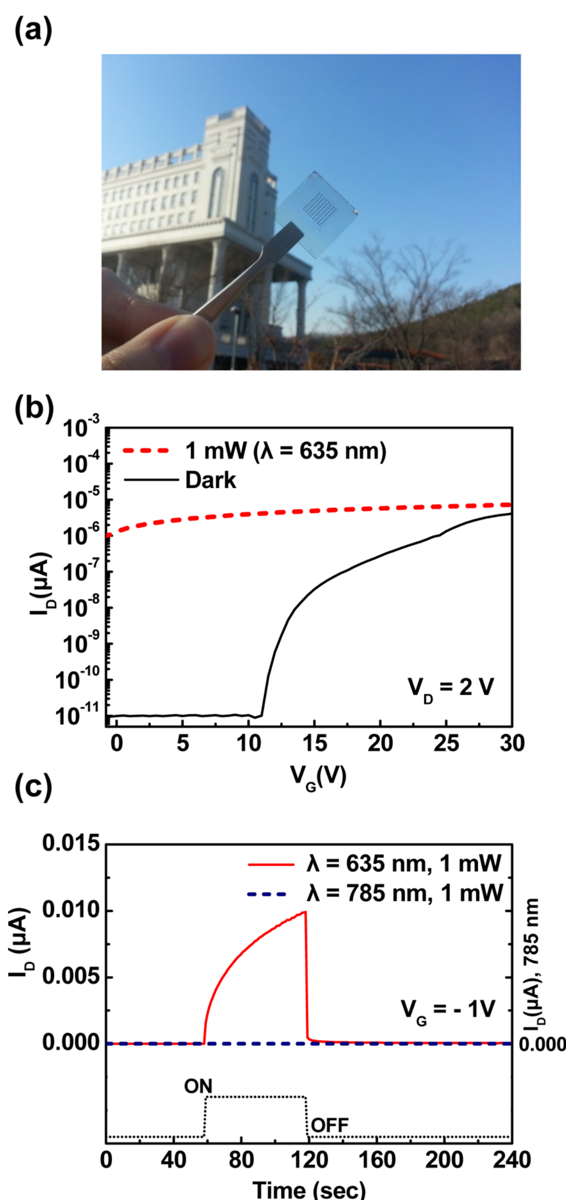

Figure 5. (a) Photograph of the phototransistor based on QDs and IGZO on a transparent glass substrate. (b) Transfer characteristics of the device with and without light illumination. (c) Time-resolved photocurrent with pulses of the laser source (λ = 635 and 785 nm).

DOI: 10.1021/acsami.5b04683
ACS Appl. Mater. Interfaces 2015, 7, 19666−19671

were placed between IGZO and the Al_2O_3 gate insulator. The source−drain electrodes were formed with 100 nm of aluminum. The transfer characteristics of the device with and without laser illumination (λ = 635 nm) are shown in Figure 5b. In the presence of visible-light illumination, the photocurrent dramatically increased with small applied gate and drain voltages. The time-resolved photocurrent with a pulse of laser (λ = 635 and 785 nm) is shown in Figure 5c. As expected, the device responded to 635 nm laser illumination because of the small band gap of the QDs. However, the photon (λ = 785 nm) with a smaller energy than the band gap of the QDs could not induce the photocurrent. These results indicate that highly transparent photodetectors with high photoresponsivity to visible light can be fabricated using wide-band-gap oxide semiconductors and small-band-gap QDs.

4. CONCLUSION

Visible-light phototransistors were fabricated using a hybrid active channel material based on IGZO and QDs. A wide-band-gap IGZO film was used as a transparent semiconducting channel, while small-band-gap QDs were adopted to absorb and induce the photocurrent under visible-light illumination. The photons of the visible light were absorbed by the QDs, which excited the electrons from the valence to the conduction bands of QDs. The electrons in the conduction band of QDs are then easily injected into the conduction band of IGZO to induce a photocurrent. The device shows good photoresponsivity and responds to the high frequency of a visible-light signal that is not visible to the human eye. A transparent device on a glass substrate with QDs at the interface between IGZO and Al_2O_3 was also demonstrated. Therefore, the results suggest that highly transparent, visible-light photodetectors can be developed using oxide semiconductors and QDs as an active semiconducting material.

■ ASSOCIATED CONTENT

Supporting Information

The Supporting Information is available free of charge on the ACS Publications website at DOI: 10.1021/acsami.5b04683.

> Transfer and output characteristics of IGZO and QD-decorated IGZO transistors with exposure of a red laser (λ = 635 nm) according to changes in the thickness of the IGZO film, transfer characteristics of the QD device without a IGZO semiconducting channel, and transfer characteristics and time-resolved photocurrent of IGZO transistors, where QDs were placed at the interface of IGZO and SiO_2 (PDF)

■ AUTHOR INFORMATION

Corresponding Author

*Tel/Fax: +82 31 201 3324. E-mail: junkang@khu.ac.kr (S.J.K.).

Notes

The authors declare no competing financial interest.

■ ACKNOWLEDGMENTS

This work was supported by the Center for Advanced Soft-Electronics funded by the Ministry of Science, ICT and Future Planning as a Global Frontier Project (CASE-2014M3A6A5060946). It was also supported by a grant from the National Research Foundation of Korea (Grant NRF-2013R1A1A1A05007934). We thank Dr. Y. H. Kim for support with the TEM measurements.

■ REFERENCES

(1) Takechi, K.; Nakata, M.; Azuma, K.; Yamaguchi, H.; Kaneko, S. Dual-Gate Characteristics of Amorphous $InGaZnO_4$ Thin-Film Transistors as Compared to Those of Hydrogenated Amorphous Silicon Thin-Film Transistors. *IEEE Trans. Electron Devices* **2009**, *56*, 2027−2033.

(2) Sakai, T.; Seo, H.; Aihara, S.; Kubota, M.; Egami, N.; Wang, D.; Furuta, M. A 128 × 96, 50 μm Pixel Pitch Transparent Readout Circuit Using Amorphous In−Ga−Zn−O Thin-Film Transistor Array with Indium-Tin Oxide Electrodes for an Organic Image Sensor. *Jpn. J. Appl. Phys.* **2012**, *51*, 010202.

(3) Chen, W.-T.; Zan, H.-W. High-Performance Light-Erasable Memory and Real-Time Ultraviolet Detector Based on Unannealed Indium-Gallium-Zinc-Oxide Thin-Film Transistor. *IEEE Electron Device Lett.* **2012**, *33*, 77−79.

(4) Jeong, J. K.; Jeong, J. H.; Yang, H. W.; Park, J.-S.; Mo, Y.-G.; Kim, H. D. High Performance Thin Film Transistors with Cosputtered Amorphous Indium Gallium Zinc Oxide Channel. *Appl. Phys. Lett.* **2007**, *91*, 113505.

(5) Nomura, K.; Ohta, H.; Takagi, A.; Kamiya, T.; Hirano, M.; Hosono, H. Room-Temperature Fabrication of Transparent Flexible Thin-Film Transistors Using Amorphous Oxide Semiconductors. *Nature* **2004**, *432*, 488−492.

(6) Kim, K.; Choi, K.-Y.; Lee, H. a-InGaZnO Thin-Film Transistor-Based Operational Amplifier for an Adaptive DC-DC Converter in Display Driving System. *IEEE Trans. Electron Devices* **2015**, *62*, 1189−1194.

(7) Jeon, S.; Ahn, S.-E.; Song, I.; Kim, C. J.; Chung, U.-I.; Lee, E.; Yoo, I.; Nathan, A.; Lee, S.; Ghaffarzadeh, K.; Robertson, J.; Kim, K. Gated Three-Terminal Device Architecture to Eliminate Persistent Photoconductivity in Oxide Semiconductor Photosensor Arrays. *Nat. Mater.* **2012**, *11*, 301−305.

(8) Chang, T. H.; Chiu, C. J.; Chang, S. J.; Tsai, T. Y.; Yang, T. H.; Huang, Z. D.; Weng, W. Y. Amorphous InGaZnO Ultraviolet Phototransistors with Double-Stacked Ga_2O_3/SiO_2 Dielectric. *Appl. Phys. Lett.* **2013**, *102*, 221104.

(9) Chang, T. H.; Chiu, C. J.; Weng, W. Y.; Chang, S. J.; Tsai, T. Y.; Huang, Z. D. High Responsivity of Amorphous Indium Gallium Zinc Oxide Phototransistor with Ta_2O_5 Gate Dielectric. *Appl. Phys. Lett.* **2012**, *101*, 261112.

(10) Zan, H.-W.; Chen, W.-T.; Hsueh, H.-W.; Kao, S.-C.; Ku, M.-C.; Tsai, C.-C.; Meng, H.-F. Amorphous Indium-Gallium-Zinc-Oxide Visible-Light Phototransistor with a Polymeric Light Absorption Layer. *Appl. Phys. Lett.* **2010**, *97*, 203506.

(11) Park, S. J.; Lee, S. M.; Kang, S. J.; Lee, K.-H.; Park, J.-S. Plasmon-Enhanced Photocurrent of Ge-Doped InGaO Thin Film Transistors Using Silver Nanoparticles. *J. Vac. Sci. Technol., A* **2015**, *33*, 021101.

(12) Liu, X.; Yang, X.; Liu, M.; Tao, Z.; Dai, Q.; Wei, L.; Li, C.; Zhang, X.; Wang, B.; Nathan, A. Photo-Modulated Thin Film Transistor Based on Dynamic Charge Transfer within Quantum-Dots-InGaZnO Interface. *Appl. Phys. Lett.* **2014**, *104*, 113501.

(13) Jasieniak, J.; Califano, M.; Watkins, S. E. Size-Dependent Valence and Conduction Band-Edge Energies of Semiconductor Nanocrystals. *ACS Nano* **2011**, *5*, 5888−5902.

(14) Lee, S. M.; Park, S. J.; Lee, K. H.; Park, J.-S.; Park, S.; Yi, Y.; Kang, S. J. Enhanced Photocurrent of Ge-Doped InGaO Thin Film Transistors with Quantum Dots. *Appl. Phys. Lett.* **2015**, *106*, 031112.

(15) Gadre, M. J.; Alford, T. L. Highest Transmittance and High-Mobility Amorphous Indium Gallium Zinc Oxide Films on Flexible Substrate by Room-Temperature Deposition and Post-Deposition Anneals. *Appl. Phys. Lett.* **2011**, *99*, 051901.

(16) Lee, Y.; Omkaram, I.; Park, J.; Kim, H.-S.; Kyung, K.-U.; Park, W.; Kim, S. A a-Si:H Thin-Film Phototransistor for a Near-Infrared Touch Sensor. *IEEE Electron Device Lett.* **2015**, *36*, 41−43.

(17) Ozel, T.; Gaur, A.; Rogers, J. A.; Shim, M. Polymer Electrolyte Gating of Carbon Nanotube Network Transistors. *Nano Lett.* **2005**, *5*, 905−911.

DOI: 10.1021/acsami.5b04683
ACS Appl. Mater. Interfaces 2015, 7, 19666−19671